Comparison of Non-Coding RNAs in Exosomes and Functional Efficacy of Human Embryonic Stem Cell-versus Induced Pluripotent Stem Cell-Derived Cardiomyocytes

WON HEE LEE,[a,b,*] WEN-YI CHEN,[a,b,*] NING-YI SHAO,[a,b] DAN XIAO,[a,b] XULEI QIN,[a,b] NATALIE BAKER,[a,b] HYE RYEONG BAE,[a,b] TZU-TANG WEI,[a,b] YONGJUN WANG,[a,b] PRAVEEN SHUKLA,[a,b] HAODI WU,[a,b] KAZUKI KODO,[a,b] SANG-GING ONG,[a,b] JOSEPH C. WU [a,b,c]

Key Words. Stem cells • Exosomes • Cell therapy • Embryonic stem cell-derived cardiomyocyte • Induced pluripotent stem cell-derived cardiomyocyte

[a]Stanford Cardiovascular Institute, [b]Departments of Medicine and Radiology, and [c]Institute of Stem Cell Biology and Regenerative Medicine, Stanford University School of Medicine, Stanford, California, USA

*W.H.L. and W.Y.C. contributed equally to this work.

S.-G.O., J.C.W serve as Co-Senior authors for this manuscript.

Correspondence: Joseph C. Wu, M.D., Ph.D., 265 Campus Drive G1120B, Stanford, California 94305-5454, USA. Telephone: 650-736-2246; Fax: 650-736-0234; e-mail: joewu@stanford.edu; or Sang-Ging Ong, Ph.D., 1291 Welch Road. Grant S114, Stanford, California 94305-5111, USA. Telephone: 650-736-2863; Fax: 650-723-6272; e-mail: sang-ging@stanford.edu

ABSTRACT

Both human embryonic stem cell-derived cardiomyocytes (ESC-CMs) and human induced pluripotent stem cell-derived CMs (iPSC-CMs) can serve as unlimited cell sources for cardiac regenerative therapy. However, the functional equivalency between human ESC-CMs and iPSC-CMs for cardiac regenerative therapy has not been demonstrated. Here, we performed a head-to-head comparison of ESC-CMs and iPSC-CMs in their ability to restore cardiac function in a rat myocardial infarction (MI) model as well as their exosomal secretome. Human ESCs and iPSCs were differentiated into CMs using small molecule inhibitors. Fluorescence-activated cell sorting analysis confirmed ~85% and ~83% of CMs differentiated from ESCs and iPSCs, respectively, were positive for cardiac troponin T. At a single-cell level, both cell types displayed similar calcium handling and electrophysiological properties, with gene expression comparable with the human fetal heart marked by striated sarcomeres. Sub-acute transplantation of ESC-CMs and iPSC-CMs into nude rats post-MI improved cardiac function, which was associated with increased expression of angiogenic genes in vitro following hypoxia. Profiling of exosomal microRNAs (miRs) and long non-coding RNAs (lncRNAs) revealed that both groups contain an identical repertoire of miRs and lncRNAs, including some that are known to be cardioprotective. We demonstrate that both ESC-CMs and iPSC-CMs can facilitate comparable cardiac repair. This is advantageous because, unlike allogeneic ESC-CMs used in therapy, autologous iPSC-CMs could potentially avoid immune rejection when used for cardiac cell transplantation in the future. STEM CELLS 2017;35:2138–2149

SIGNIFICANCE STATEMENT

Although both embryonic stem cell-derived cardiomyocytes (ESC-CMs) and induced pluripotent stem cells-derived CMs (iPSC-CMs) have been studied for cardiac repair, a direct comparison between both cell types in terms of therapeutic efficacy would be helpful to the field. In this study, we compared both ESC-CMs and iPSC-CMs at a single-cell level and showed that both cell types displayed similar calcium handling and electrophysiological properties, with comparable gene expression to human fetal heart, with striated sarcomeres. Importantly, injection of both cell types subacutely following myocardial infarction in a rat model demonstrated these cells to facilitate comparable therapeutic recovery. We have also shown that both ESC-CMs and iPSC-CMs produce exosomes and have characterized the non-coding RNA repertoire of these exosomes.

INTRODUCTION

Myocardial infarction (MI) and subsequent ischemic heart failure are the major causes of mortality and morbidity worldwide. Although a number of preclinical and clinical studies have used various types of cells such as bone marrow cells, skeletal muscle cells, and mesenchymal stem cells [1], currently no therapy can fully replace the cardiomyocytes (CMs) lost after MI and other cardiomyopathies. As a possible alternative, transplanting human embryonic stem cell-derived CMs (ESC-CMs) in animals has demonstrated at least partial functional restoration and cell engraftment [2–5]. More recently, Menasche et al. reported a human clinical trial using human ESC-derived cardiac progenitor

cells [6]. Therefore, exogenous transplantation of ESC-CMs represents a promising future therapeutic strategy.

One potential complication of ESC-CMs in clinical studies is immune rejection, which may be circumvented using induced pluripotent stem cells (iPSCs) generated from the same patients [7]. iPSCs are somatic cells reprogrammed to become pluripotent. Similar to ESCs, iPSCs can self-renew and differentiate into all somatic cell types [8–10]. Unlike ESCs, iPSCs are derived from mature somatic cells, which underwent reprogramming events via reintroduction of embryonic genes. However, previous studies have shown that human ESCs and iPSC have distinct gene expression profiles [11, 12]. Therefore, the question as to whether ESC-CMs and iPSC-CMs are equivalent therapeutically must be answered before iPSC-CMs can be used as an alternative to ESC-CMs.

To address this question, we directly compared the therapeutic efficacy of both cell types by transplanting them into ischemic rat hearts and measured cardiac function by magnetic resonance imaging (MRI). We found that ESC-CMs and iPSC-CMs not only have similar sarcomere structures, gene expression, calcium and electrophysiological properties but also promote cardiac repair equally. In addition, we investigated exosomes produced by both groups of CMs by microRNA (miR) and long non-coding RNA (lncRNA) profiling because exosomes have been shown to be involved in cardiac repair [13]. Interestingly, our results revealed an identical composition of highly abundant miRs and lncRNAs even though they came from two distinct pluripotent cell types, suggesting the specificity of exosomal RNAs is dependent on the differentiated cell type.

MATERIALS AND METHODS

An expanded Methods section is available in the Supporting Information Experimental Procedures.

Study Design and Animal Surgery

CMs derived from human ESCs and iPSCs were characterized and cryopreserved on day 30 after the differentiation started. MI was introduced by ligating the left anterior descending coronary artery in adult athymic nude rats under anesthesia (2% inhaled isoflurane) by an experienced microsurgeon. Cells were transplanted 4 days after MI. All rats underwent MRI 1 day before transplantation to establish the baseline of cardiac function and also 1 month after transplantation. Rats were randomized into three groups receiving (a) transplantation of 1×10^7 ESC-CMs ($n = 8$), (b) transplantation of 1×10^7 iPSC-CMs ($n = 8$), and (c) phosphate-buffered saline (PBS) as control ($n = 7$). Cells were injected at two sites in the peri-infarct zone with a total volume of ~40 μl of PBS per injection site using a 28-gauge insulin syringe. The hearts were harvested for histological analysis after completing the MRI 1 month following transplantation.

Culture, Maintenance, and Differentiation of Pluripotent Stem Cells

Both pluripotent stem cell types were cultured, maintained, and differentiated as described previously [14]. Human iPSCs and ESCs were cultured in E8 media (Gibco, NY, http://www.thermofisher.com) with daily media replenishment. Cells were replated using 0.5 mM EDTA at 1:10 or 1:12 ratios every 4 days, at which time they reached ~85% confluence. During differentiation, cells were treated for 2 days with 6 μM CHIR99021 (Selleck Chemicals, TX, http://www.selleckchem.com) in RPMI+B27 supplement without insulin. On day 2, cells were placed on RPMI+B27 without insulin and CHIR99021. On days 3–4, cells were treated with 5 μM IWR-1 (Selleck Chemicals, TX, http://www.selleckchem.com). On days 5–6, cells were removed from IWR-1 treatment and placed on RPMI+B27 without insulin. From day 7 onward, cells were placed on RPMI+B27 with insulin until beating was observed.

Flow Cytometry

Cells were dissociated into single cells using TrypLE (Gibco, NY, www.thermofisher.com) for 5 minutes at 37°C, pelleted, and fixed in cytofix/cytoperm (BD Biosciences, CA, www.bdbiosciences.com) for 10 minutes at 4°C. Cells were then incubated with 1:100 anti-cTnT antibody (Thermo Scientific, NY, www.thermofisher.com MS-295-P), 1:100 CD31 (Dako, Denmark, www.agilent.com M082329–2), fibroblast surface protein 1 (FSP-1; Millipore, CA, www.emdmillipore.com 07–2274), alpha smooth muscle actin (SMA; Abcam, United Kingdom, www.abcam.com ab32575), or their isotype control, followed by incubation with secondary antibodies conjugated with Alexa 647 (Thermo Fisher, NY, www.thermofisher.com) (Supporting Information Table S3). Every incubation step was performed in cytoperm/cytowash (BD Biosciences, CA, www.bdbiosciences.com). Samples were run on a BD flow cytometer and analyzed using the FlowJo software.

Calcium Imaging of ESC-CMs and iPSC-CMs

Spontaneous Ca^{2+} transients were recorded at 37°C using a single-cell line scan mode. Regions of interest were delineated in each video frame and analyzed for changes in dye intensity F/F_0, in which F_0 is the resting fluorescence value at the first frame of each video. Total Ca^{2+} release or release dynamics was calculated using IgorPro 6.22. Transient amplitude was expressed as $\Delta F/F_0$. Decay Tau (mS) was calculated by mono exponential curve fitting.

Electrophysiology

Whole cell action potentials were recorded with the use of standard patch-clamp technique, as described previously [14]. More details are provided in Supporting Information Materials.

Total RNA Isolation, Reverse Transcription, and Quantitative Real-Time PCR

Cells were washed with PBS and harvested in Trizol (Qiagen, Germany, www.qiagen.com). The human fetal heart sample (18 weeks gestation) was obtained from StemExpress, CA, www.stemexpress.com. The study was approved by the Stanford Institutional Review Board. Total RNA isolation was performed using a miRNeasy kit (Qiagen). RNA was eluted in water and stored at −80°C. RNA concentration was measured using UV spectrophotometry at 260 nm (Nanodrop, Thermo Fisher, NY, www.thermofisher.com) and the purity was determined with the 260A/280A ratio. cDNA was obtained using the high capacity cDNA Reverse Transcription Kit (Thermo Fisher, NY, http://www.thermofisher.com) with random hexamer primers. TaqMan assays for the real-time polymerase chain reaction (PCR) were purchased from Applied Biosystems. TaqMan assays for the real-time PCR (Thermo Fisher, NY, www.thermofisher.com) are listed in Supporting Information Table S4. Quantitative real-time PCR for each

sample was performed in triplicates using the StepOnePlus system (Applied Biosystems Thermo Fisher, NY, www.thermofisher.com). Fold-differences were normalized to GAPDH and calculated using the $2^{-\Delta\Delta Ct}$ method.

Cardiac MRI

MRI was performed 1 day before and 30 days after cell or PBS delivery using a preclinical 7T (MR901 Discovery) horizontal bore scanner (Agilent Technologies, CA, www.agilent.com) with a shielded gradient system (600 mT/m) as described previously [15]. For more details, refer Supporting Information Materials.

Immunohistochemistry and Histology

Immunofluorescence and histological analyses were performed using standard protocols. For more details, refer to Supporting Information Table S5.

Exosome Isolation from Normoxic and Hypoxic CMs

For each batch of exosome isolation, a total of 2.4×10^7 ESC-CMs or iPSC-CMs were seeded onto six-well plate (2×10^6 cells in 2 ml of media per well). For normoxia, CMs were grown in RPMI-1640 media supplemented with B27 supplement minus antioxidants for 36 hours, after which the supernatant was collected for exosome isolation. The same batch of cells were then cultured in RPMI-1640 glucose-free media supplemented with B27 supplement minus antioxidants, and then placed in hypoxic pouches (BD GasPak EZ Anaerobe Pouch System, BD Biosciences, CA, www.bdbiosciences.com) for 36 hours, after which the supernatant was collected. For exosome isolation, both normoxic and hypoxic supernatant were centrifuged at 400 g for 10 minutes, before being filtered through a 0.22-μm device to remove apoptotic bodies [16]. Filtered supernatant was then concentrated approximately 20 times using 100 kDa filters (Amicon Ultra-15, Millipore), before being incubated with 0.5 volumes of Total Exosome Isolation Reagent (Thermo Fisher, NY, www.thermofisher.com) and incubated at 4°C overnight. The supernatant/reagent mixture was then centrifuged at 10,000 g for an hour at 4°C before discarding the supernatant, and the exosome-containing pellet was collected for subsequent experiments.

miR Sequencing

Exosomal RNA was isolated using a miRCURY RNA Isolation Kit (Exiqon, Denmark, www.exiqon.com) according to manufacturer's protocol. Total RNA of each sample was used to prepare the miRNA sequencing library, which included the following steps: (a) 3' adapter ligation; (b) 5' adapter ligation; (c) cDNA synthesis; (d) PCR amplification; and (e) size selection of ~130–150 bp PCR amplified fragments (corresponding to ~15–35 nt small RNAs). The libraries were denatured as single-stranded DNA molecules, captured on Illumina flow cells, amplified in situ as clusters and finally sequenced for 36 cycles on Illumina HiSeq per the manufacturer's instructions. The clean reads that passed the quality filter were processed to remove the adaptor sequence as the trimmed reads. Trimmed reads were aligned to the miRBase pre-miRNAs. miRNA read counts were normalized as tag counts per million miRNA alignments (TpM).

Statistical Analysis

Experimental results are expressed as mean ± SEM. Two-tailed Student's t test was used to calculate significant differences in the ejection fractions of the groups (ESC-CMs, iPSC-CMs, and PBS control). Multiple comparison correction analysis was performed using an analysis of variance and post-hoc Tukey's honestly significant difference test. Differences were considered significant at $p < .05$.

RESULTS

Generation and Differentiation of CMs Derived from Human ESCs and iPSCs

A schematic overview of the study is summarized in Supporting Information Figure S1. Human iPSCs were generated from human adult dermal fibroblasts by lentiviral-mediated transduction of Oct4, Sox2, Klf4, and c-Myc. To compare ESCs and iPSCs, we used the ESC H7 line as comparison. Human ESCs and iPSCs were maintained and differentiated as described previously [14]. Approximately 2 weeks after the induction of differentiation, most of the cells began to contract. Flow cytometry analysis of representative cultures at day 30 indicated that CMs made up ~85% of the total population as measured by cTnT$^+$ staining (Fig. 1A), whereas only a small number of cells stained positive for CD31, FSP, or SMA, markers for endothelial cells, fibroblasts, and smooth muscle cells, respectively (Supporting Information Fig. S2). At this point, the cells were enzymatically dissociated from the plates and cryopreserved in liquid nitrogen.

ESC-CMs and iPSC-CMs Shared Comparable Sarcomeric Structures, Cardiac Gene Expression Profile, and Ca^{2+} Handling Properties

To evaluate the expression of myofilament proteins and the sarcomeric organization in ESC-CMs and iPSC-CMs, immunostaining with antibodies against cTnT (a highly cardiac specific myofilament protein) and sarcomeric alpha actinin (present at the Z-line of the sarcomere) was performed (Fig. 1B). A clear striated pattern for sarcomeric alpha actinin staining was observed in both ESC-CMs and iPSC-CMs. Both ESC-CMs and iPSC-CMs presented a comparable morphology in terms of sarcomeric length, cell perimeter, multinucleation, and surface area (Fig. 1C). Collectively, immunofluorescence staining of myofilament proteins indicated that sarcomeric structures were similarly developed in ESC-CMs and iPSC-CMs. Next, we compared the gene expression in ESC-CMs and iPSC-CMs, as well as fetal human myocardium, by quantitative real-time PCR using a panel of cardiac markers that included calcium handling (*CASQ2*), gap junction (*GJA5*), potassium channel (*KCNJ2*, *KCNJ5*), structural genes (*MYH6*, *MYH7*), and sodium channel (*SCN5A*) markers. The expression of these genes in ESC-CMs and iPSC-CMs was comparable with that of human fetal myocardium (Fig. 1D). For example, the expression of *KCNJ5*, *MYH6*, and *MYH7* was similar, and the expression of *CASQ2*, *GJA5*, and *KCNJ2* in ESC-CMs and iPSC-CMs was within twofold range of human fetal myocardium's expression level. To assess the contractility of ESC-CMs and iPSC-CMs, we next measured Ca^{2+} transients using the ratiometric dye Fura-2. Peak transient amplitude, maximal upstroke, decay velocities, time to peak, and Ca^{2+} reuptake (as measured by the time to 50% relaxation) were all identical (Fig. 1E). Both ESC-CMs and iPSC-CMs displayed similar maturity for calcium handling (transient amplitude: $\Delta F/F_0 = 3.8 \pm 0.3$; time to peak: ~200 ms; transient duration: ~750 ms; 50% transient duration:
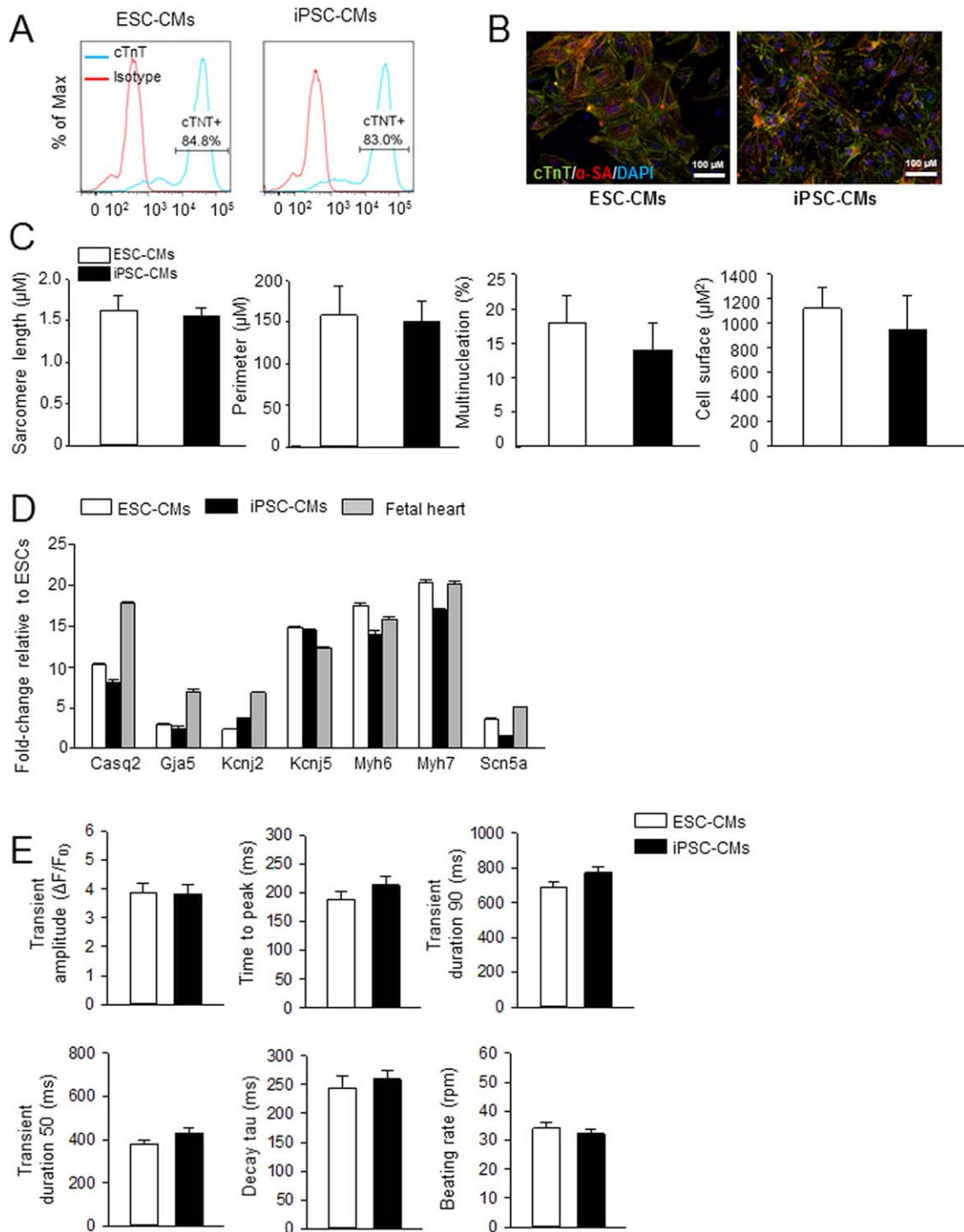
Figure 1. Cardiomyocytes (CMs) derived from human embryonic stem cells (ESCs) and induced pluripotent stem cells (iPSCs) with high purity and displayed cardiac phenotype. **(A):** Cardiac differentiation of human ESCs and iPSCs. Representative flow cytometry analysis at day 30 indicated that the total cell population consisted of ∼85% CMs as measured by cardiac troponin T (cTnT$^+$) staining. **(B):** Fixed and stained cells were imaged using fluorescence microscopy and quantitatively analyzed. Scale bar = 100 μM. **(C):** Comparable structures of ESC-CMs and iPSC-CMs in sarcomere length, cell perimeter, percentage of multinucleated cells, and cell surface area (mean ± SEM; n = 30–40 cell per cell line). **(D):** Quantitative real-time polymerase chain reaction showed that calcium handling gene (*CASQ2*), gap junction (*GJA5*), potassium channel (*KCNJ2* and *KCNJ5*), structural genes (*MYH6* and *MYH7*), and sodium channel (*SCN5A*) were present in human ESC-CMs and iPSC-CMs at similar levels as those for human fetal heart tissue (mean ± SEM; n = 3 independent experiments). **(E):** Ca^{2+} transient of ESC-CMs and iPSC-CMs was measured using ratiometric dye Fura-2. Both ESC-CMs and iPSC-CMs displayed similar maturity in calcium handling (transient amplitude: $\Delta F/F_0$ = 3.8 ± 0.3; time to peak: ∼200 ms; transient duration: ∼750 ms; 50% transient duration: ∼400 ms; decay tau: ∼250 ms) (mean ± SEM; n = 15–20 cells from three independent experiments). Abbreviations: CM, cardiomyocyte; cTNT, cardiac troponin T; DAPI, 4′,6-diamidino-2-phenylindole; ESC, embryonic stem cell; iPSC, induced pluripotent stem cell; SA, sarcomeric actin.

~400 ms; decay tau: ~250 ms). To assess the action potential characteristics, patch clamping around days 33–38 demonstrated a heterogeneous phenotype, with ventricular-like cells being the predominant phenotype (ESC-CMs: 55% with an MDP of −66.1 mV; iPSC-CMs: 62% with an MDP of −67.8 mV) along with atrial-like and nodal-like cells (Supporting Information Fig. S3; Table S1). Both ESC-CMs and iPSC-CMs have similar ratios of nodal-like (18% and 15%), atrial-like (27% and 23%), and ventricular-like CMs (55% and 62%). Taken together, these results demonstrated that CMs derived from human ESCs and iPSCs are relatively similar at molecular and cellular levels.

Comparable Functional Improvement of Cardiac Function in Rats Injected with Either ESC-CMs or iPSC-CMs

It has been reported that human ESC-CMs engraft but do not alter cardiac remodeling or improve cardiac function in a rat model of chronic MI where cells were injected at 1 month following ischemia-reperfusion [3]. We, therefore, focused on whether transplantation of ESC-CMs and iPSC-CMs would have therapeutic effects on the recipient hearts using a subacute MI model instead where cells were injected at 4 days post-MI (Fig. 2A). MRI was performed 1 day before cell transplantation to establish the baseline and to exclude the animals without sufficient infarct (ejection fraction (EF) >60%), thus ensuring that all three groups have comparable infarct sizes before cell transplantation or control surgery (Supporting Information Fig. S4). Transplantation of ESC-CMs ($n = 8$), iPSC-CMs ($n = 8$), or PBS ($n = 7$; control group) was performed 4 days after MI. The overall experimental design is outlined in Supporting Information Figure S1. All three groups showed a progressive ventricular dilation relative to their baseline (Fig. 2A). While end-diastolic volumes were not significantly different among the three groups (Fig. 2B), end-systolic volume increased significantly in the PBS control group ($p = .03$; Fig. 2C). The difference is better illustrated by comparing the changes in EF for each group (Fig. 2D, 2E). The EF was improved by 4.8% ± 1.8% and 6.3% ± 2.1% for ESC-CM and iPSC-CM groups, respectively (Fig. 2E). By contrast, the EF declined in PBS control group by 4.6% ± 1.6% (Fig. 2E). A summary of all parameters measured via MRI is found in Supporting Information Table S2.

Immunofluorescence Staining Confirms the Engraftment of ESC-CMs and iPSC-CMs in Ischemic Rat Hearts

To assess the engraftment of transplanted ESC-CMs and iPSC-CMs, the infarcted rat hearts were harvested after 1 month and the engraftment was assessed by immunofluorescence staining. Human β-integrin staining demonstrated engraftment of ESC-CMs (Fig. 3A, 3B) and iPSC-CMs (Fig. 3C, 3D) in the myocardium 1 month after injection. Staining with sarcomeric alpha actinin revealed that ESC-CMs (Fig. 3E, 3F) and iPSC-CMs (Fig. 3G, 3H) maintained a CM-like morphology after injection. However, staining of the gap junction protein, Connexin 43, only showed sporadic distribution within the graft, suggesting that most injected CMs did not form proper gap junctions within this time period (Fig. 3A–3D). Staining of CD31, which is expressed on the endothelium of blood vessels, showed that the grafts were likely perfused by the blood vessels present in the grafts (Fig. 3E–3H). As human-derived cardiomyocytes beat significantly slower compared to a rat heart, [4], it is unlikely that the improvement of ejection fraction resulted from the direct contribution to the

contractility by ESC-CMs or iPSC-CMs. An alternative explanation may be that human CMs release paracrine factors that promote angiogenesis and reduce apoptosis in the setting of ischemia, accounting for the functional benefit and attenuated cardiac remodeling that were observed (Supporting Information Fig. S5). To explore this hypothesis, we next investigated the pro-angiogenic and anti-apoptotic potential by using a simulated ischemic environment assay under real-time quantitative PCR. Human ESC-CMs and iPSC-CMs subjected to in vitro ischemia showed a significantly increased expression of pro-angiogenic and survival factors (e.g., vascular endothelial growth factor [*VEGF*], angiopoietin 1 [*ANG1*], and epidermal growth factor [*EGF*] but not fibroblast growth factor [*FGF2*]) compared with control conditions (Fig. 3I). These results indicated that human ESC-CMs and iPSC-CMs could provide a framework that support new vessel growth and protect against cell death via secretion of paracrine factors, and thus better preserve host myocardium (e.g., via reduced fibrosis) (Supporting Information Fig. S5). This premise is corroborated by CD31 staining showing that host blood vessels grew into the grafts (Fig. 3E–3H).

miR Profiling of Exosomes Derived from Human ESC-CMs and iPSC-CMs

As a variety of stem cell types have been reported to release paracrine factors in the form of membrane vesicles, we next sought to study exosomes released by human ESC-CMs and iPSC-CMs under normoxic versus hypoxic conditions. Both ESC-CMs and iPSC-CMs were found to secrete exosomes under normoxic conditions as characterized by immunoblotting for exosomal markers CD63 and CD81 (Fig. 4A) as well as by transmission electron microscopy (Fig. 4B). miR sequencing yielded ~13 million reads for ESC-CM-derived exosomes (ESC-CM-Exo) and ~11 million reads for iPSC-CM-derived exosomes (iPSC-CM-Exo), respectively. After quality and length filtering, ~12 million reads in ESC-CM-Exo and ~10 million reads in iPSC-CM-Exo were used for further analysis (data not shown). Principal component analysis revealed four distinct miRNAs profiles (Fig. 4C). Interestingly, the effects of hypoxia on the relative abundance of top 20 annotated miRNAs compared to normoxia were negligible for both ESC-CM-Exo and iPSC-CM-Exo (Table 1), including several miRs associated with cardioprotection (e.g., miR-1, miR-21, and miR-30) [17–19]. Importantly, a comparable profile of abundant miRNAs was observed in exosomes isolated from another line of ESC-CMs and iPSC-CMs, demonstrating the specificity of exosomal miRNAs packaging in stem cell-derived CMs (Supporting Information Fig. S6; Table S6). Interestingly, upon exposure to hypoxia, the numbers of miRs that were differentially expressed (both up- and down-regulated) were lower in iPSC-CM-Exo compared with ESC-CM-Exo (Fig. 4D, 4E). Functional annotation using gene ontology (GO) analysis based on abundant miRs found in ESC-CM-Exo and iPSC-CM-Exo was subsequently performed (Fig. 4F, 4G).

lncRNA Profiling of Exosomes Derived from Human ESC-CMs and iPSC-CMs

To better characterize the secretome of ESC-CM-Exo and iPSC-CM-Exo, we next investigated the expression profile of lncRNAs and related mRNAs of normoxic ESC-CM-Exo and iPSC-CM-Exo. Volcano plot filtering found 135 lncRNAs and 65 mRNAs to be higher in iPSC-CM-Exo compared with ESC-CM-Exo, and 72 lncRNAs and 46 mRNAs were lower in iPSC-CM-Exo compared with ESC-CM-Exo (Fig. 5A, 5B).
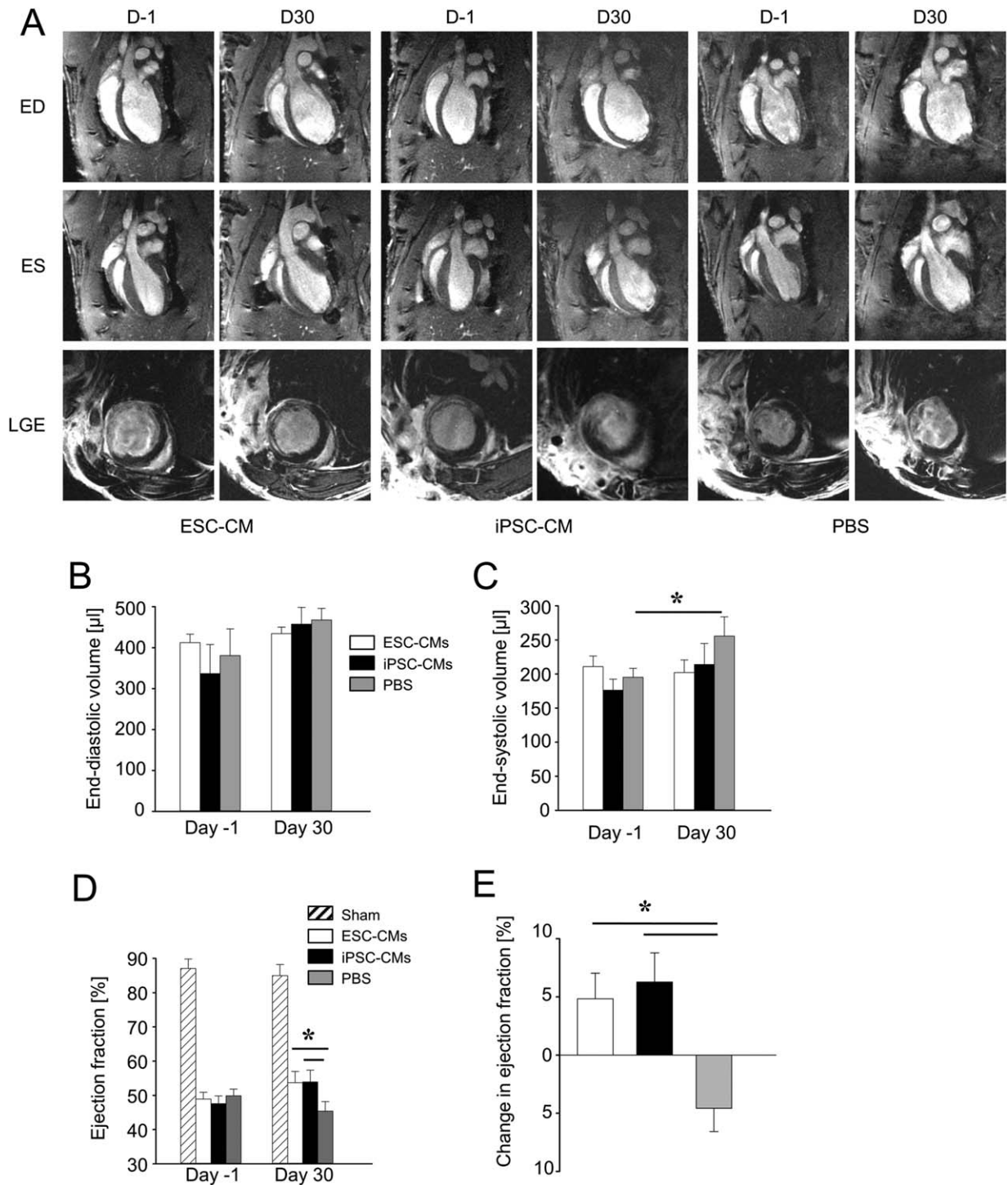
Figure 2. Magnetic resonance imaging (MRI) data showed comparable functional improvements of cardiac functions of rats injected with embryonic stem cell (ESC)-derived cardiomyocytes (CMs) and induced pluripotent stem cell (iPSC)-derived CMs. Quantitative MRI was used to assess left-ventricular ejection fractions of ischemic rats receiving ESC-CMs ($n = 8$), iPSC-CMs ($n = 8$), or phosphate-buffered saline (PBS) ($n = 7$). **(A):** The top row shows representative two-chamber long-axis views at end-diastole 1 day before (D–1) and 30 days after (D30) cell implantation or PBS. The middle row shows the same hearts at end-systole, whereas the bottom row shows corresponding late gadolinium enhancement images at mid-ventricular level. **(B):** End-diastolic volumes increased in all groups but were not significantly different. **(C):** End-systolic volumes increased significantly in the PBS group (mean $\pm$ SEM; $p = .03$), but the increases were not significant in ESC-CM and iPSC-CM groups. **(D, E):** Ejection fractions increased in ESC-CM and iPSC-CM groups but declined in the PBS group (mean $\pm$ SEM; $p = .03$). Abbreviations: CM, cardiomyocyte; ED, end-diastole; ES, end-systole; ESC, embryonic stem cell; iPSC, induced pluripotent stem cell; LGE, late gadolinium enhancement; PBS, phosphate-buffered saline.
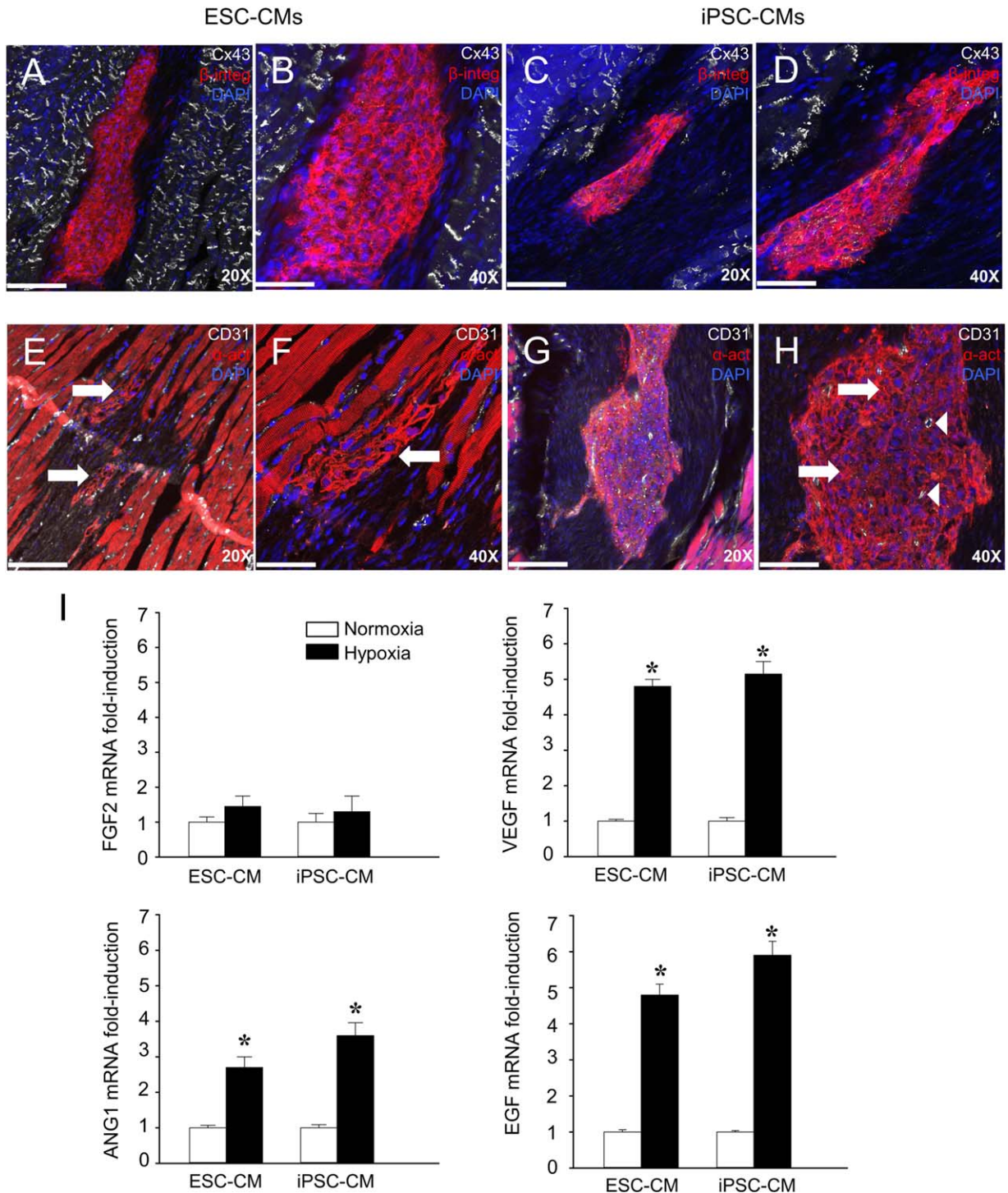
Figure 3. Immunofluorescence images of grafted embryonic stem cell (ESC)-derived cardiomyocytes (CMs) and induced pluripotent stem cell (iPSC)-derived CMs post transplantation in ischemic rat hearts. One month after cell injection, grafts were found in the border zone. The grafts were typically separated from the host myocardium by scar tissue. **(A–D):** Grafts that stained positive for human beta integrin 1 (β-Integ) were found in the hearts given cell injection, with minimal cell junctions that stained positive for connexin 43 (Cx43). **(E–H):** Grafts were positive for sarcomeric alpha actinin (α-act) and displayed striated sarcomeric structure as indicated by arrows. CD31 staining (arrow heads) revealed that the grafts were perfused by blood vessels that had grown into the graft. Scale bars = (A, C, E, G) 100 μm; (B, D, F, H) 50 μm. **(I):** Gene expression analysis revealed that ESC-CMs and iPSC-CMs under ischemic conditions significantly increased expression of vascular endothelial growth factor, angiopoietin-1 (ANG1), and endothelial growth factor compared with the normoxia condition (mean ± SEM, $p < .05$ from four independent experiments) but not fibroblast growth factor-2. Abbreviations: CM, cardiomyocyte; DAPI, 4′,6-diamidino-2-phenylindole; ESC, embryonic stem cell; iPSC, induced pluripotent stem cell. FGF2, fibroblast growth factor2; VEGF, vascular endothelial growth factor; EGF, epidermal growth factor.
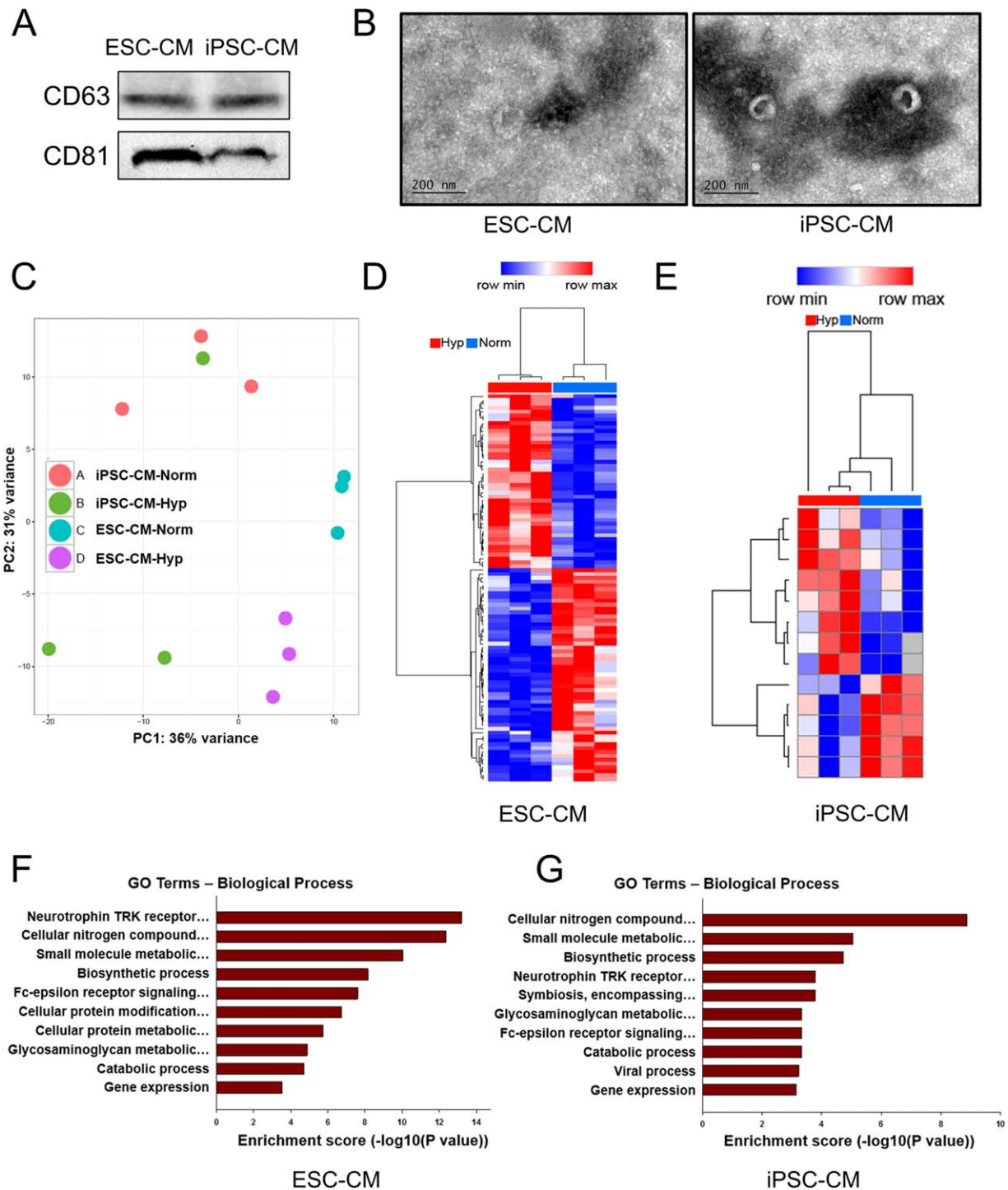
Figure 4. microRNA profiling of exosomes harvested from embryonic stem cell (ESC)-derived cardiomyocytes (CMs) and induced pluripotent stem cell (iPSC)-derived CMs under normoxic and hypoxic conditions. **(A, B):** Characterization of exosomes by immunoblotting of exosomal markers and transmission electron microscopy. **(C):** Principal component analysis of exosomal miRs under four different conditions. **(D, E):** Heat map of differentially expressed miRs in both ESC-CM-Exo and iPSC-CM-Exo under hypoxic condition compared with control (normoxic condition). **(F, G):** Gene ontology analysis of abundant miRNAs in both ESC-CMs and iPSC-CMs. Abbreviations: CM, cardiomyocyte; ESC, embryonic stem cell; GO, gene ontology; iPSC, induced pluripotent stem cell.

Hierarchical clustering also showed a distinctive lncRNA and gene expression profiling between ESC-CM-Exo and iPSC-CM-Exo (Fig. 5C). Interestingly, similar to miRNAs, the profile of abundant lncRNAs between ESC-CM-Exo and iPSC-CM Exo was also highly similar (Supporting Information Table S7). A complete list of differentially expressed lncRNAs and mRNAs between ESC-CM-Exo and iPSC-CM-Exo is attached separately as Supporting Information (Supporting Information Tables S8, S9). GO enrichment analysis of differentially expressed mRNAs

Table 1. Top 20 abundant exosomal miRNAs

ESC-CM normoxia	ESC-CM hypoxia	iPSC-CM normoxia	iPSC-CM hypoxia
hsa-miR-novel-chr18_20848	hsa-miR-1–3p	hsa-miR-novel-chr18_20848	hsa-miR-1–3p
hsa-miR-1–3p	hsa-miR-novel-chr18_20848	hsa-miR-1–3p	hsa-miR-novel-chr18_20848
hsa-miR-143–3p	hsa-miR-143–3p	hsa-miR-143–3p	hsa-miR-143–3p
hsa-miR-30d-5p	hsa-miR-30d-5p	hsa-miR-148a-3p	hsa-miR-21–5p
hsa-miR-148a-3p	hsa-miR-27b-3p	hsa-miR-30d-5p	hsa-miR-30d-5p
hsa-miR-novel-chr9_61538	hsa-miR-148a-3p	hsa-miR-novel-chr9_61538	hsa-miR-378a-3p
hsa-miR-100–5p	hsa-miR-100–5p	hsa-miR-378a-3p	hsa-miR-148a-3p
hsa-miR-21–5p	hsa-miR-21–5p	hsa-miR-21–5p	hsa-miR-27b-3p
hsa-miR-99a-5p	hsa-miR-378a-3p	hsa-miR-99b-5p	hsa-miR-99a-5p
hsa-miR-27b-3p	hsa-miR-99a-5p	hsa-miR-99a-5p	hsa-miR-26a-5p
hsa-miR-378a-3p	hsa-miR-novel-chr9_61538	hsa-miR-27b-3p	hsa-miR-99b-5p
hsa-miR-99b-5p	hsa-miR-26a-5p	hsa-miR-151a-3p	hsa-miR-novel-chr9_61538
hsa-miR-novel-chrX_63253	hsa-miR-novel-chr3_39325	hsa-miR-92a-3p	hsa-miR-92a-3p
hsa-miR-novel-chrY_65063	hsa-miR-99b-5p	hsa-miR-320a	hsa-miR-novel-chr3_39325
hsa-miR-92a-3p	hsa-miR-92a-3p	hsa-miR-30a-5p	hsa-miR-191–5p
hsa-miR-320a	hsa-miR-374b-5p	hsa-miR-191–5p	hsa-miR-30a-5p
hsa-miR-423–3p	hsa-miR-151a-3p	hsa-miR-100–5p	hsa-miR-151a-3p
hsa-miR-151a-3p	hsa-let-7g-5p	hsa-miR-novel-chrX_63253	hsa-let-7g-5p
hsa-miR-26a-5p	hsa-miR-133a-3p	hsa-miR-novel-chrY_65063	hsa-miR-125a-5p
hsa-miR-125a-5p	hsa-miR-30c-5p	hsa-miR-125a-5p	hsa-miR-novel-chr5_49778

between both groups implicated various processes including cell migration and tissue development (Fig. 5D).

DISCUSSION

Recent advances in differentiating CMs from pluripotent stem cells using a small molecule differentiation protocol has enabled the generation of highly pure CMs (>85%) from ESCs and iPSCs, thus preventing possible complications resulting from heterogeneous cell populations and making it possible to directly compare the efficacy of ESC-CMs and iPSC-CMs in cell transplantation therapy. The most important observation in this study is that the transplantation of iPSC-CMs into ischemic rat hearts attenuated the cardiomyopathy progression after initial MI to the same extent as ESC-CM transplantation, and hence could provide a viable solution to the problem of immune rejection associated with ESC therapy in the future. Although both ESC-CM and iPSC-CM groups showed similar end-diastolic volume as the PBS group, the increase in end-systolic volume of left ventricle chamber was less profound in both ESC-CM and iPSC-CM groups compared with PBS group, suggesting the preservation of cardiac function by cell injection. Importantly, the ejection fraction increased significantly in both ESC-CM and iPSC-CM groups at day 30 by ~5% compared with day −1. By contrast, the ejection fraction in the PBS group continued to deteriorate.

Despite their positive influence on post-MI cardiac modeling, the transplanted CMs still appeared phenotypically immature. Although the transplanted cells maintained CM morphology as shown by sarcomeric alpha actinin staining, they were separated from the host myocardium by scar tissues and their sarcomere structures were not as well organized as adult CMs. Furthermore, connexin 43 staining suggests that most of the transplanted cells were not electrically coupled. Therefore, it is unlikely that the beneficial effects were provided by the contractile force generated by transplanted cells. A more plausible scenario is that the host cells were influenced indirectly by paracrine factors secreted from the transplanted cells. Indeed, previous studies [20, 21] and the data we presented here show that the transplanted CMs could secrete paracrine factors that may enhance angiogenesis,

improve the extracellular matrix, or modulate the immune response, thus improving survival of host myocardium. Importantly, we have demonstrated that both ESC-CMs and iPSC-CMs are capable of secreting exosomes, which are known to transfer a wide range of active biomolecules, including mRNA, miRNAs, lncRNAs, proteins, and lipids, making them key modulators of the intercellular communication network.

As previous studies have demonstrated that hypoxic preconditioning of cells before transplantation enhances their therapeutic potential, we hypothesized that the miRNA expression profile will be altered upon in vitro exposure of ESC-CMs and iPSC-CMs to hypoxia. Interestingly, the 20 most abundant miRNAs in both ESC-CM-Exo and iPSC-CM-Exo were found to be similar regardless of exposure to hypoxia or normoxia, suggesting the strong presence of a cell type-specific miRNA packaging system. Among these miRNAs, several have been reported to be cardioprotective, including miR-1, miR-21, and miR-30 [17–19]. In addition, we observed that although exposure to hypoxia led to the differential expression of selected miRNAs (including miR-210 and cardioprotective miR-133) in ESC-CM-Exo, these effects were markedly blunted in iPSC-CM-Exo, reflecting subtle differences between the two cell types. Similarly, the contents of lncRNAs between exosomes from both groups of cells were also highly similar.

Although we do not fully understand why the transplanted CMs failed to reach maturity, we speculate three possible reasons. The first possibility is species differences, as we transplanted human CMs into rat hearts with a normal beating rate of >400 beats per minutes compared with a normal human heart rate of <100 beats per minutes. In fact, when CMs were transplanted in slower heart-rate animals such as pigs [20], monkeys [5], or guinea pigs [4], they have been reported to electrically couple with host CMs. Second, the cells we transplanted are less mature compared with adult CMs, which is reflected in cell morphology, Ca^{2+} transient, and electrophysiology. Therefore, they might need stimuli from the ideal microenvironment or more time to become mature. Third, the huge number of dying cells in the injection sites may induce unfavorable host responses and result in a hostile environment for cells to survive. Therefore, although we showed that iPSC-CMs could serve as a viable source for cell transplantation therapy, protocols to further
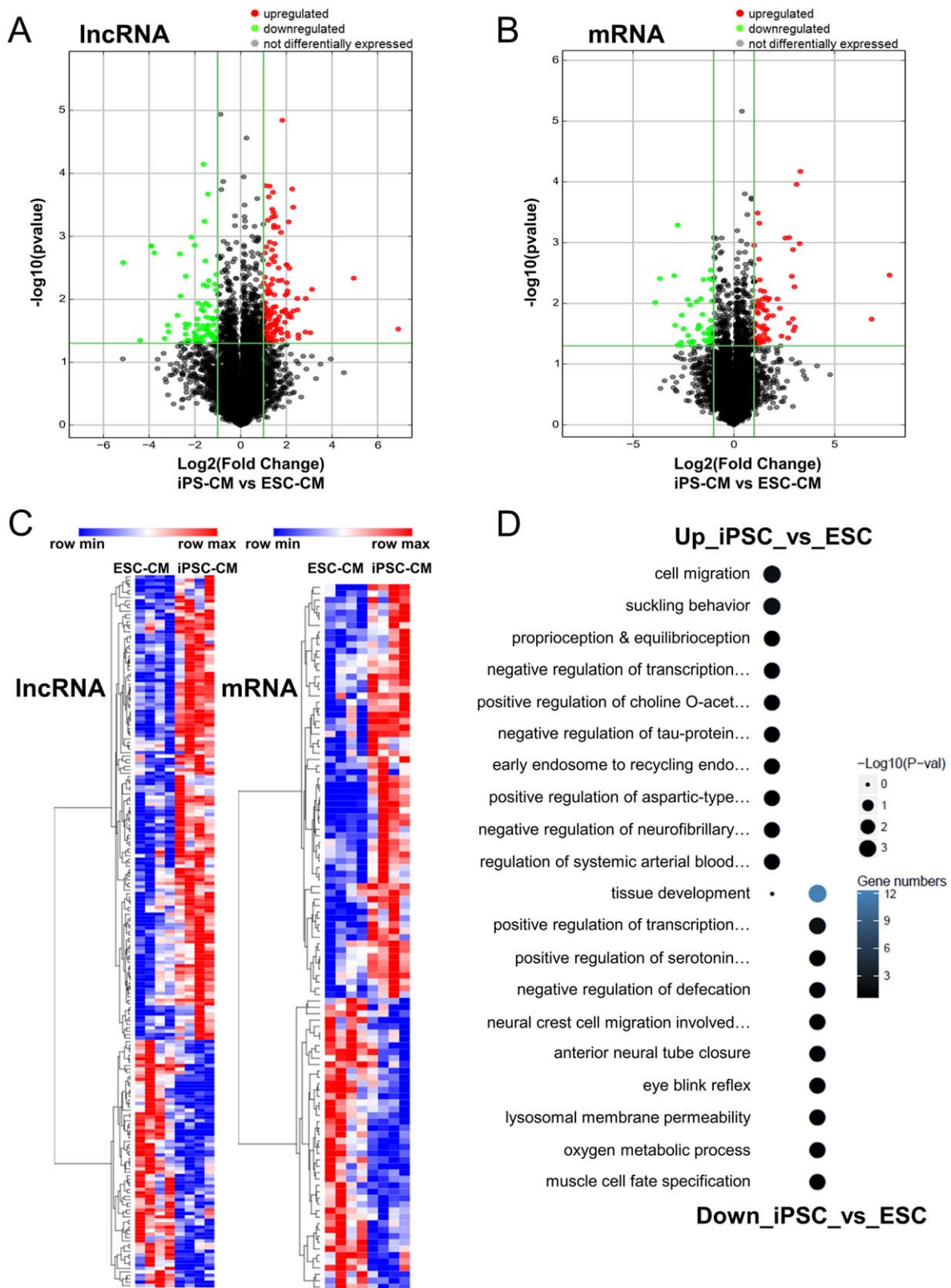
Figure 5. LncRNA and mRNA profiling of normoxic exosomes harvested from embryonic stem cell (ESC)-derived cardiomyocytes (CMs) and induced pluripotent stem cell (iPSC)-derived CMs. **(A, B):** Volcano plot of differentially expressed lncRNA (left) and mRNA (right) between iPSC-CMs and ESC-CMs. **(C):** Hierarchical clustering of lncRNAs and mRNAs between iPSC-CMs and ESC-CMs. **(D):** Gene ontology analysis of biological processes based on upregulated and downregulated genes between iPSC-CMs and ESC-CMs. Microarray data from this study have been deposited to the GEO database under the accession number GSE100218. Abbreviations: CM, cardiomyocyte; ESC, embryonic stem cell; iPSC, induced pluripotent stem cell.

mature CMs and methods to minimize cell death during delivery will be required to fully assess the efficacy of cell transplantation therapy. In addition, further work is needed to determine the optimal maturation state of to-be-transplanted CMs for maximal therapeutic efficacy. Various methods have been described to improve the maturity of both ESC-CMs and iPSC-CMs, including prolonged culture, substrate stiffness, cell patterning, electrical stimulation, and biochemical cues. Immature cells may have a higher proliferative capacity that may be beneficial in the context of replacing damaged myocardium, and these cells are relatively resistant to ischemia and oxidative stress. However, these cells may also present a proarrhythmic risk following transplantation due to their automaticity. In addition, immature CMs are associated with a weaker contractile force and lack mature excitation–contraction coupling, both of which could limit their functional contractile output in the infarcted myocardium. As this study investigated only the functional efficacy of day 30 ESC-CMs versus iPSC-CMs, future studies are warranted to investigate different maturation states or differentiation timing for comparison with achieve maximal regenerative efficacy.

It has been shown that iPSCs can induce an immune response [22], but the immunogenicity can be drastically reduced after differentiation into specific lineages [23–25]. Therefore, iPSC derivatives remain a better alternative than ESC derivatives to avoid the complications from immune rejection. Furthermore, significant progress has been made on nonintegration methods to generate iPSCs [26], which will make iPSC derivatives even more ideal as candidates for cell replacement therapy in the future.

CONCLUSION

In summary, our study demonstrated that transplantation of both ESC-CMs and iPSC-CMs provided comparable functional recovery, with cells engrafted but not electrically coupled a month after transplantation. We also demonstrated that CMs from both groups are capable of producing exosomes that harbor similar miRs. Collectively, our study indicates that autologous transplantation of iPSC-CMs may be an attractive alternative to allogenic transplantation of ESC-CMs in the future.

AUTHOR CONTRIBUTIONS

W.H.L., W.Y.C., and S.-G.O.: conception and design, collection and/or assembly of data, data analysis and interpretation, manuscript writing; N.-Y.S.: sequencing data analysis and interpretation; D.X., N.B., H.R.B., T.-T.W., Y.W., and K.K.: collection and/or assembly of data; X.Q., P.S., and H.W.: collection and/or assembly of data, data analysis and interpretation; J.C.W.: conception and design, financial support, data analysis and interpretation, manuscript writing, final approval of manuscript.

DISCLOSURE OF POTENTIAL CONFLICTS OF INTEREST

The authors indicated no potential conflicts of interest.

REFERENCES

1 Matsa E, Sallam K, Wu JC. Cardiac stem cell biology: Glimpse of the past, present, and future. Circ Res 2014;114:21–27.

2 Laflamme MA, Chen KY, Naumova AV et al. Cardiomyocytes derived from human embryonic stem cells in pro-survival factors enhance function of infarcted rat hearts. Nat Biotechnol 2007;25:1015–1024.

3 Fernandes S, Naumova AV, Zhu WZ et al. Human embryonic stem cell-derived cardiomyocytes engraft but do not alter cardiac remodeling after chronic infarction in rats. J Mol Cell Cardiol 2010;49:941–949.

4 Shiba Y, Fernandes S, Zhu WZ et al. Human ES-cell-derived cardiomyocytes electrically couple and suppress arrhythmias in injured hearts. Nature 2012;489:322–325.

5 Chong JJ, Yang X, Don CW et al. Human embryonic-stem-cell-derived cardiomyocytes regenerate non-human primate hearts. Nature 2014;510:273–277.

6 Menasche P, Vanneaux V, Hagege A et al. Human embryonic stem cell-derived cardiac progenitors for severe heart failure treatment: First clinical case report. Eur Heart J 2015;36:2011–2017.

7 Neofytou E, O'Brien CG, Couture LA, et al. Hurdles to clinical translation of human induced pluripotent stem cells. J Clin Invest 2015;125:2551–2557.

8 Takahashi K, Yamanaka S. Induction of pluripotent stem cells from mouse embryonic and adult fibroblast cultures by defined factors. Cell 2006;126:663–676.

9 Yu J, Vodyanik MA, Smuga-Otto K et al. Induced pluripotent stem cell lines derived from human somatic cells. Science 2007;318:1917–1920.

10 Wernig M, Meissner A, Foreman R et al. In vitro reprogramming of fibroblasts into a pluripotent ES-cell-like state. Nature 2007;448:318–324.

11 Chin MH, Mason MJ, Xie W et al. Induced pluripotent stem cells and embryonic stem cells are distinguished by gene expression signatures. Cell Stem Cell 2009;5:111–123.

12 Narsinh KH, Plews J, Wu JC. Comparison of human induced pluripotent and embryonic stem cells: Fraternal or identical twins? Mol Ther 2011;19:635–638.

13 Yellon DM, Davidson SM. Exosomes: Nanoparticles involved in cardioprotection? Circ Res 2014;114:325–332.

14 Burridge PW, Matsa E, Shukla P et al. Chemically defined generation of human cardiomyocytes. Nat Methods 2014;11:855–860.

15 Ong SG, Huber BC, Lee WH et al. Microfluidic single-cell analysis of transplanted human induced pluripotent stem cell-derived cardiomyocytes after acute myocardial infarction. Circulation 2015;132:762–771.

16 Ong SG, Lee WH, Huang M et al. Cross talk of combined gene and cell therapy in ischemic heart disease: Role of exosomal microRNA transfer. Circulation 2014;130:S60–S69.

17 He B, Xiao J, Ren AJ et al. Role of miR-1 and miR-133a in myocardial ischemic postconditioning. J Biomed Sci 2011;18:22.

18 Gu GL, Xu XL, Sun XT et al. Cardioprotective effect of microRNA-21 in murine myocardial infarction. Cardiovasc Ther 2015;33:109–117.

19 Roca-Alonso L, Castellano L, Mills A et al. Myocardial MiR-30 downregulation triggered by doxorubicin drives alterations in beta-adrenergic signaling and enhances apoptosis. Cell Death Dis 2015;6:e1754.

20 Ye L, Chang YH, Xiong Q et al. Cardiac repair in a porcine model of acute myocardial infarction with human induced pluripotent stem cell-derived cardiovascular cells. Cell Stem Cell 2014;15:750–761.

21 Nguyen PK, Neoftyou E, Rhee JW et al. Potential strategies to address the major clinical barriers facing stem cell regenerative therapy for cardiovascular disease: a review. JAMA Cardiol 2016;1: 953–962.

22 Zhao T, Zhang ZN, Rong Z et al. Immunogenicity of induced pluripotent stem cells. Nature 2011;474:212–215.

23 Araki R, Uda M, Hoki Y et al. Negligible immunogenicity of terminally differentiated cells derived from induced pluripotent or embryonic stem cells. Nature 2013;494:100–104.

24 Guha P, Morgan JW, Mostoslavsky G et al. Lack of immune response to differentiated cells derived from syngeneic induced pluripotent stem cells. Cell Stem Cell 2013;12:407–412.

25 de Almeida PE, Meyer EH, Kooreman NG et al. Transplanted terminally differentiated induced pluripotent stem cells are accepted by immune mechanisms similar to self-tolerance. Nat Commun 2014;5:3903.

26 Gonzalez F, Boue S, Izpisua Belmonte JC. Methods for making induced pluripotent stem cells: Reprogramming a la carte. Nat Rev Genet 2011;12:231–242.

See www.StemCells.com for supporting information available online.